scientific reports

Check for updates

OPEN

Limocitrin induced cellular death through ERK pathways in human oral squamous cell cancer

Bharath Kumar Velmurugan[1], Chia-Chieh Lin[2], Min-Yun Kao[2], Hsin-Yu Ho[2], Yu-Sheng Lo[2], Yi-Ching Chuang[2] & Ming-Ju Hsieh[2,3,4,5]✉

This study sought to investigate the anticancer efficacy of limocitrin on two distinct human oral cancer cell lines. At first, we evaluated the effect of limocitrin on the proliferation of OSCC cells (SCC-9 and SCC-47) using MTT and colony formation assays. Limocitrin treatment increased cell cycle arrest at G2/M phase, induced caspase-related apoptosis (cleaved caspase-3, caspase-8, caspase-9 and PARP expression) in OSCC cells. Limocitrin treatment inhibited Bcl-2 and Bcl-XL and induced Bax, Bak expression in both SCC-9 and SCC-47 cell lines. Limocitrin treatment inhibited cyclin E1, E2, CDK2, CDK4, and CDK6 and increased p21 expression. Limocitrin also exhibited an inhibitory effect on the phosphorylation of AKT, ERK1/2 and JNK in a dose-dependent manner. Additionally, pretreatment of oral cancer cells with U0126 resulted in increased cleaved caspase-3 and caspase-8 and PARP expression. Furthermore, limocitrin treatment decreased XIAP, cIAP1, HSP27 protein expression than control group. Combined treatment with limocitrin and si-XIAP significantly increased cleaved PARP, caspase-3 and -8 expressions in SCC-9 cells. Overall, this evidence indicates that limocitrin may serve as an effective anticancer agent for the treatment of oral cancer.

Keywords Limocitrin, OSCC, Apoptosis, ERK, AKT, JNK, Mitochondria

Abbreviations

OSCC	Oral squamous cell carcinoma
MAPK	Mitogen-activated protein kinase
JNK	C-Jun N-terminal kinase
ERK	Extracellular signal-regulated kinase

Oral squamous cell carcinoma (OSCC) is the most prevalent form of oral cancer, accounting for 96% of all cases[1]. The majority of OSCC patients are identified while they are in stages III and IV[2]. The incidence of OCSCC among young adults (YA) less than 44 years of age has increased, according to epidemiological studies[3]. Radiation therapy and chemotherapy are currently the primary treatments for OSCCs[4]. Nevertheless, those treatments have several adverse effects on healthy tissues and cells, which restrict their application in the management of cancer. Therefore, finding more effective chemotherapy medications is critically needed.

Mitogen-Activated Protein Kinase (MAPK) family comprises of majority of the signaling cascades that mediate the death of tumor cells[5]. The well-known MAPK subfamily proteins are p38 kinase, c-Jun N-terminal kinase (JNK), and Extracellular Signal-regulated Kinase (ERK). JNK promotes apoptosis through two different mechanisms[6].

Limocitrin a hydroxyflavan (Fig. 1A), is a natural compound (isolated from *P. acerifolia* and *P. orientalis* buds[7]. Limocitrin exerts anticancer activity against breast cancer[8] and NK leukemia[9] cell lines. According to earlier research, limocitrin limits the growth of breast cancer cells by suppressing cell survival factors such as AKT, Bcl-2, Bid, mTOR, PI3K, procaspases, and p70 S6 kinase, as well as by upregulating the expression of proteins linked to apoptosis[8]. Limocitrin's ability to prevent cancer in OSCC cells hasn't been thoroughly studied yet. Thus, in this work, we employed an in vitro model to investigate the cytotoxic effects of limocitrin and the molecular mechanism that underlies them in human OSCC cells.

[1]Maitocon Laboratory, Tirupur 641604, India. [2]Oral Cancer Research Center, Changhua Christian Hospital, Changhua 50006, Taiwan. [3]Graduate Institute of Clinical Medicine, College of Medicine, National Chung Hsing University, Taichung 402202, Taiwan. [4]Doctoral Program in Tissue Engineering and Regenerative Medicine, College of Medicine, National Chung Hsing University, Taichung 402, Taiwan. [5]Graduate Institute of Biomedical Sciences, China Medical University, Taichung 404, Taiwan. ✉email: 170780@cch.org.tw

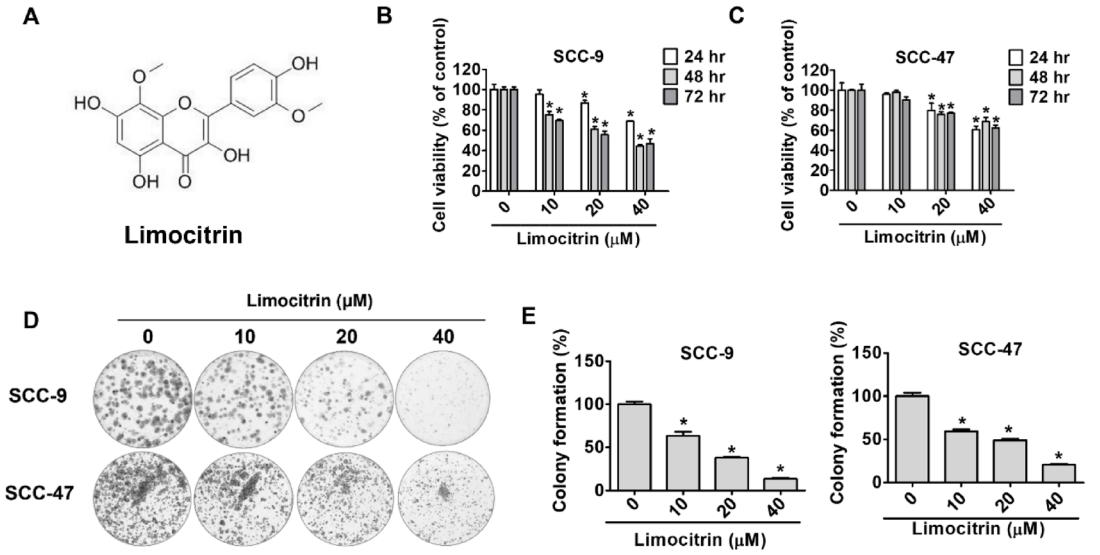

Fig. 1. The cytotoxicity of limocitrin against two oral cancer cell lines. (**A**) Chemical structure of limocitrin. (**B**) Treatment effects on SCC-9 and (**C**) SCC-47 cells with limocitrin (0, 10, 20, and 40 μM) for 24, 48, and 72 h. (**D**) Colony formation in SCC-9 and SCC-47 cells following Limocitrin treatment. (**E**) Quantitative analysis of colony formation, with counts obtained using a stereomicroscope. All data are presented as mean ± standard deviation (n = 3). *$p < 0.05$, indicating statistical significance compared with the control group.

Materials and methods

Cell culture

Human OSCC cell lines SCC-47 and SCC-9 were selected for experimentation. The cell lines were purchased from the Japanese Collection of Research Bioresource Cell Bank (Shinjuku, Japan). SCC-47 and SCC-9 were cultured in Dulbecco's Modified Eagle Medium (DMEM) (Life Technologies, Grand Island, NY, USA)/F12. The culture media was supplemented with 10% fetal bovine serum (FBS), 10,000 U/ml penicillin and 10 mg/mL streptomycin. All cell lines were maintained at 37 °C in a humidified atmosphere of 5% CO_2.

Cell proliferation and cytotoxicity assay

To assess cell viability, we used the Cell Counting Kit-8 (CCK-8) assay. We seeded the two oral cancer cell lines on 96-well plates (1×10^4 cells/well) and cultured them for 24 h at 37 °C. Subsequently, we treated the cells with different concentrations of limocitrin (0, 10, 20, and 40 μM) in the culture media supplemented with 10% FBS for periods of 24, 48, and 72 h. After treatment, we added CCK-8 solution to each well and incubated the samples. We then measured the absorbance at a wavelength of 450 nm by using a microplate reader (BioTek, Winooski, VT, USA).

Colony formation assay

To evaluate the potency of limocitrin against oral cancer cells, we seeded SCC-47 and SCC-9 cells on six-well plates at the density of 5×10^3 cells/well. After incubation for 16 h at 37 °C in a 5% CO_2 atmosphere, we treated the cells with different concentrations of limocitrin (0, 10, 20, 40 μM) in the culture media supplemented with 10% FBS for 24 h. Cells were replaced with the fresh medium every 3 days, with limocitrin added. 10 days later, we washed the colony cells with phosphate-buffered saline and stained them with 0.3% crystal violet dye for 1 h and then quantified the number of colonies using a microscope.

Mitochondrial membrane potential measurement analysis

After treatment with different concentrations of limocitrin in the culture media supplemented with 10% FBS, the cells were collected and stained with Muse MitoPotential dye for 20 min at 37 °C, followed by incubation with 7-AAD for 5 min and measurement of experimental signals by Muse Cell Analyzer flow cytometry (Merck Millipore, Burlington, MA, USA), and the data were analyzed by Muse Cell Soft V1.4.0.0 Analyzer.

Western blot assay

Protein samples were extracted from the cells with lysis buffer and then separated using 10% polyacrylamide gel before transfer to polyvinylidene fluoride (PVDF) membranes (Merck Millipore). The membranes were then blocked using 5% nonfat milk prepared in a TBST buffer for 1 h and subsequently incubated with primary antibodies for 24 h at 4 °C. Subsequently, the cells were incubated for 1 h with secondary (peroxidase-conjugated) antibodies at room temperature. Finally, the membranes were then subjected to ECL detection and photographed using chemiluminescence fluorescence ImageQuant biomolecule imaging system (ChemiDoc MP (Bio-Rad)).

ImageJ was used for protein quantification. The primary antibodies against cyclin E1 #20,808, cyclin E2 #4132, p21 #2947, CDK2 #2546, CDK4 #12,790, CDK6 #3136, Fas #4233, DR5 #8074, DcR3 #4758, DcR2 #8049, Bax #5023, Bak #3814, Bcl-2 #3498, Bcl-xL #2764, c-caspase 3 #9664, c-caspase 8 #9496, c-caspase 9 #9502, c-PARP #5625, p-AKT #4060, AKT #2920, p-ERK #4370, ERK #4695, p38 #9212, p-JNK #4668, JNK #9258, XIAP #14,334, cIAP-1 #7065, HSP-27 #95,357, p-HSP-27 #9709 and β-actin #4970 were purchased from Cell Signaling Technology, Danvers, MA, USA; antibody against p-p38 #44-684G was purchased from Invitrogen, Carlsbad, MA, USA. The dilution factor of all primary antibodies was 1:1000.

Cell cycle analysis

For cell cycle analysis, cells were seeded 3×10^5 on 6-well plates and treated with limocitrin (0, 10, 20, 40 μM) in the culture media supplemented with 10% FBS for 24 h. Subsequently, we harvested the cells and fixed them in 70% ethanol at − 20 °C overnight. The fixed cells were stained with PI buffer (4 mg/ml PI, 1% Triton X-100, 0.5 mg/ml RNase A in PBS) for 30 min in the dark at room temperature. The cell cycle distribution was analyzed by Muse Cell Analyzer flow cytometry (Merck Millipore, Burlington, MA, USA), and the data were analyzed by Muse Cell Soft V1.4.0.0 Analyzer. We recorded the percentage distribution of the cells in the sub-G1, G0/G1, S, and G2/M phases.

Annexin-V/propidium iodide double staining assay

To conduct the annexin-V/propidium iodide double staining assay, we seeded cells on six-well plates (3×10^5 cells/well) and then incubated with different concentrations of limocitrin (0, 10, 20, 40 μM) in the culture media supplemented with 10% FBS for 24 h. Subsequently, the cells were suspended in PBS (2% BSA) for 15 min, we then cultured the cells and retreated them with a buffer containing annexin-V and propidium iodide. Following incubation, cell analysis was performed by Muse Cell Analyzer flow cytometry (Merck Millipore, Burlington, MA, USA), and the data were analyzed by Muse Cell Soft V1.4.0.0 Analyzer.

Nucleus staining assay

Cells in 6-well dish were fixed with methanol and stained with a blue-fluorescent DNA stain (4',6-diamidino-2-phenylindole, DAPI) after treated limocitrin in the culture media supplemented with 10% FBS for 24 h. The results were recorded by a fluorescence microscope (Leica Biosystems Division of Leica Microsystems Inc., Deerfield, IL, USA).

Proteome profiler analysis

The SCC-9 and SCC-47 cells were lysed using RIPA lysis buffer. The whole cell lysates were injected into Proteome Profiler Human Apoptosis Array kit (R&D Systems Inc., cat. ARY009; Minneapolis, MN, USA). Capture antibodies were spotted in duplicate on the nitrocellulose membrane. Target analytes were detected using a biotinylated or horseradish peroxidase (HRP)-conjugated detection antibody. The blots were visualized using ChemiDoc™ MP Imaging System (Bio-Rad, Hercules, CA, USA).

RNA interference experiments

The oral cancer cell lines were seeded onto 6-well plates with appropriate cell numbers. The Human XIAP, cIAP1 and HSP-27 siRNA (Cohesion Biosciences, London, UK) and Negative control were transfected with Turbofect reagent (Thermo Fisher Scientific; Waltham, MA, USA) dissolve in DMEM medium (FBS free). Next day, the transfected cells were treated with limocitrin (40 μM) in the culture media supplemented with 10% FBS for 24 h. The protein samples extracted from the cells were further detected by Western blot analysis.

Statistical analysis

For statistical analysis, SigmaPlot v12.5 (Grafiti LLC; Palo Alto, CA, USA) was used. We analyzed differences among subgroups using a one-way analysis of variance and Tukey's comparison test. All data are presented as mean ± standard error of the mean (n = 3). Statistical significance was set at $p < 0.05$.

Results

Limocitrin inhibits cell proliferation in OSCC

To determine the cytotoxic effect of limocitrin on human oral cancer cell lines, SCC-9 and SCC-47 cells were treated with different concentrations of limocitrin (0, 10, 20, and 40 μM) for 24, 48, and 72 h. The results indicated that limocitrin significantly inhibited the oral cancer cell viability in a concentration-dependent and time-dependent manner (Fig. 1B, C; $^*p < 0.05$). Additionally, studies for colony formation demonstrated that limocitrin treatment dramatically reduced the number of colonies in oral cancer cells (Fig. 1C; $^*p < 0.05$).

Limocitrin induces cell apoptosis by the mitochondrial pathway and the death receptor mediated mechanism

Oral cancer cells were treated with various doses of limocitrin and then analyzed for mitochondrial membrane potential to understand whether apoptosis is induced via mitochondrial pathway. As shown in Fig. 2A–C, the mitochondrial membrane potential was reduced, and the depolarized cells were increased in limocitrin treated cells. Additionally, we measured the expression levels of proteins linked to apoptosis in OSCC cells, for which we determined the expression of pro-apoptotic proteins. Figure 2D,F showed the limocitrin treatment increased pro-apoptotic proteins Bax and Bak expression and decreased anti-apoptotic protein Bcl-xL and Bcl-2 expression in oral cancer cells. In addition, limocitrin treatment increased Fas, DcR2, DcR3, and DR5 expression compared with the control group (Fig. 2E,G).

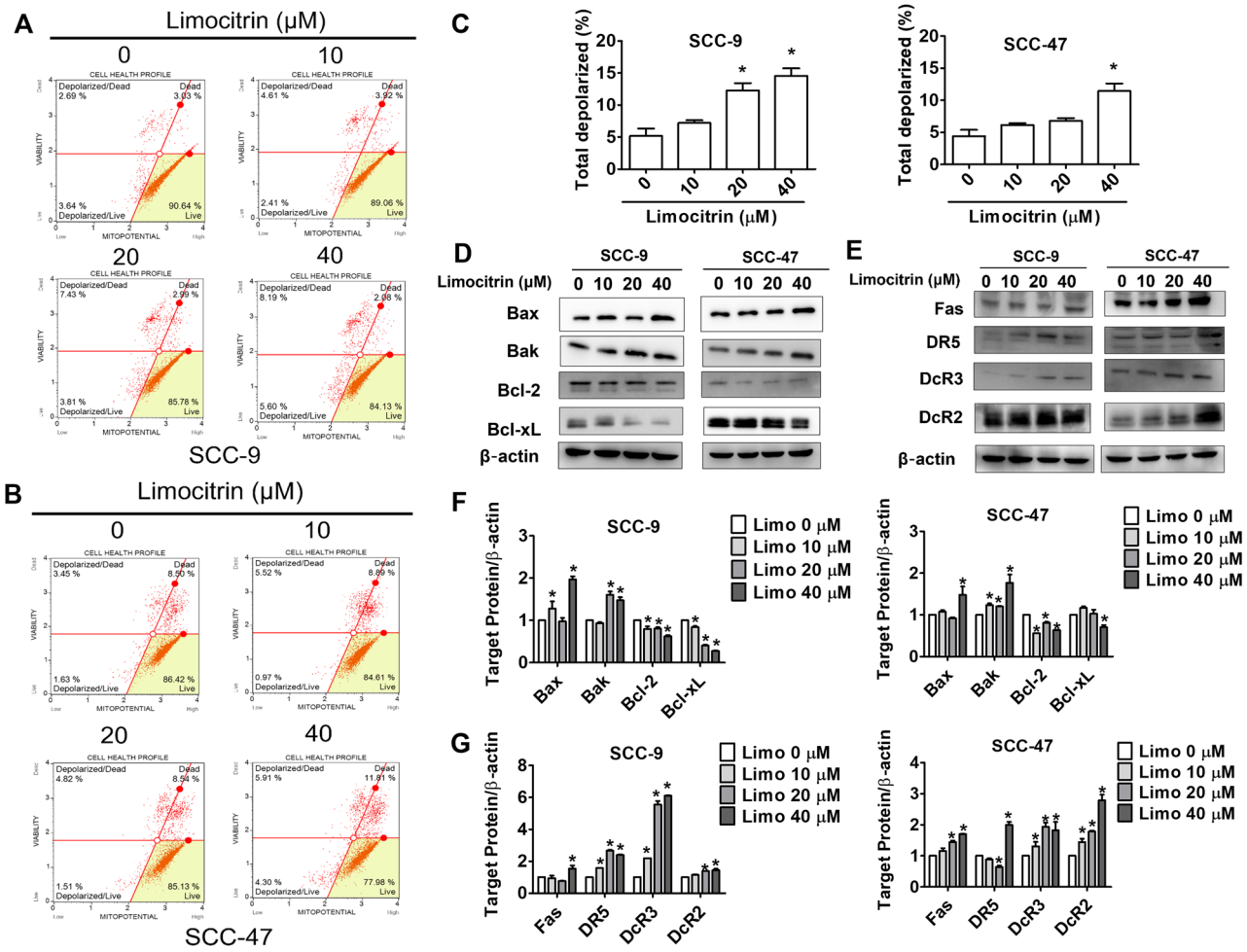

Fig. 2. Influence of limocitrin on intrinsic apoptotic pathway and mitochondrial membrane depolarization in oral cancer cells. (**A**, **B**) Flow cytometric analysis of depolarized cells in SCC-9 and SCC-47 cell lines. (**C**) Quantitation of total depolarized cells. (**D**) Western blot analysis of Bax, Bak, Bcl-2, and Bcl-XL, with β-actin as the internal control. (**E**) Western blot analysis of Fas, DR5, DcR3, and DcR2, with β-actin as the internal control. (**F**, **G**) Expression levels of apoptotic proteins associated with the intrinsic pathway in limocitrin–treated SCC-9 and SCC-47. All data are presented as mean ± standard deviation (n = 3). *$p < 0.05$, indicating statistical significance compared with the control group.

Limocitrin induces G2-M phase in OSCC

Cell cycle distribution was analyzed by flow cytometry analysis. As shown in Fig. 3A–C, limocitrin treatment increased G2/M phase cell numbers in SCC-9 and SCC-47 cells. Next, the expression level of cell cycle proteins (Cyclin E1, E2, p21, CDK2, CDK4, and CDK6) was analyzed by western blotting assay (Fig. 3D,E). Limocitrin treatment decreased Cyclin E1, E2, Cyclin E1, E2 expression and increased p21 expression in a dose-dependent manner.

Limocitrin induces apoptosis in OSCC

To verify whether apoptosis is involved in the anti-oral cancer effect of limocitrin, OSCC cells (SCC-9 and SCC-47) were treated with limocitrin for 24 h and then analyzed using an Annexin V/PI apoptosis assay kit. The apoptosis rates of OSCC cells were enhanced significantly after treatment with different doses of limocitrin (Fig. 4A,B). This result was further confirmed by chromatin condensation in limocitrin treated oral cancer cells. As shown in Fig. 4C,D, there was a significant increase in chromatin condensation in limocitrin treated group than control group. To further confirm the above results, the expression levels of apoptosis-related proteins were detected by western blotting. Limocitrin treatment induced caspase-3, -9, -8, and PARP cleavage was inhibited in Z-VAD-FMK pretreated cells (Fig. 4E–H). These results demonstrated that limocitrin leads to apoptosis in OSCC cells via activation of the caspase family.

Limocitrin inhibits AKT/ERK/ JNK signaling pathway in human oral cancer cells

To investigate the effect of limocitrin on MAPK signaling pathways, we measured the levels of AKT, ERK, p38, JNK, and their phosphorylated forms through Western blot assay. In both the SCC-9 and SCC-47 cell lines,

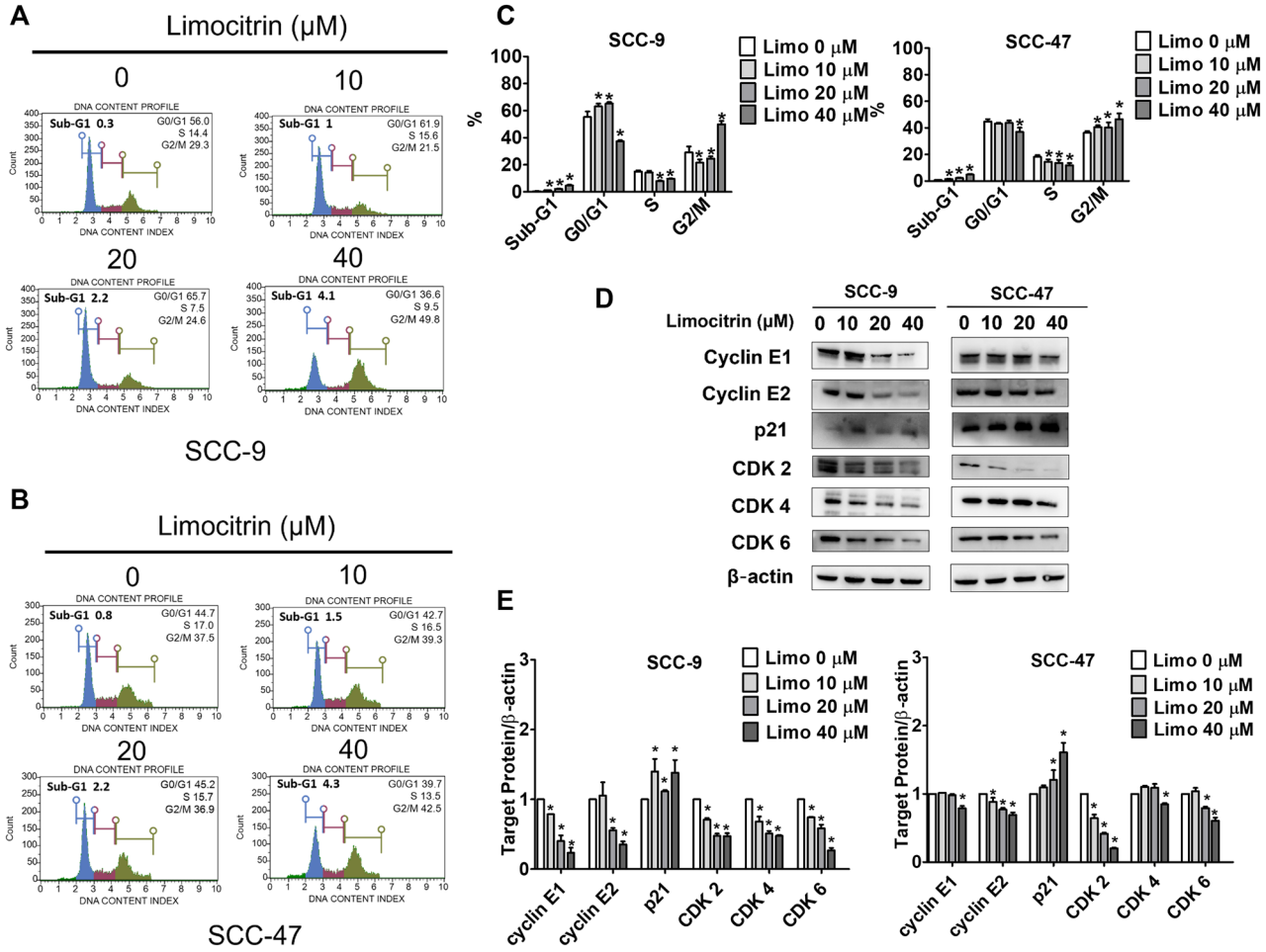

Fig. 3. Cell cycle arrest at the G2/M phase induced by limocitrin in SCC-9 and SCC-47 cell lines. (**A**, **B**) Cell cycle effects in the two oral cancer cell lines. (**C**) Quantitation of cell cycle distribution. (**D**) Western blot analysis of cell cycle-related proteins—including cyclin E1, E2, p21, CDK2, CDK4, and CDK6—with β-actin as the internal control. (**E**) Graphical representation of protein expression levels. All data are presented as mean ± standard deviation (n = 3). *$p < 0.05$, indicating statistical significance compared with the control group.

phosphorylated AKT, ERK, and JNK were downregulated after treatment with high doses of limocitrin, whereas phosphorylated p38 was upregulated after treatment with various doses of limocitrin (Fig. 5A,B). In order to determine whether limocitrin-induced apoptosis was dependent on AKT/ERK signaling pathways, cells were pre-treated with either an ERK inhibitor (U0126) or an AKT inhibitor (LY294002) for 1 h and then treated with or without limocitrin for 24 h. The results showed that cleaved PARP was slightly increased in limocitrin co-treatment with LY294002 (Fig. 5C,D) or U0126 (Fig. 5E,F) group compared with limocitrin treatment alone. Furthermore, cleaved caspase-3 was significantly increased in limocitrin co-treatment with LY294002 oral cancer cells, whereas in U0126 pretreated cells, limocitrin treatment significantly induced both cleaved caspase-3 and -8 expressions compared with the control group.

Role of XIAP in Limocitrin-induced apoptosis activation

To investigate the molecular mechanisms underlying limocitrin-induced apoptosis, we used a human apoptotic array kit. As shown in Fig. 6A, limocitrin treatment decreased XIAP, cIAP-1 and pHSP-27 expression. This result was further confirmed by dose-dependent inhibition of XIAP, cIAP-1, and pHSP-27 protein expression by western blotting (Fig. 6B). To further understand whether inhibition of these three proteins could activate the caspase pathway, we cotreated cells with or without limocitrin and si-XIAP, si-cIAP1, si-HSP27, and further analyzed for cleaved PARP, caspase-3 and -8 protein expression. Cotreatment of SCC-9 cells with specific siRNA (si-XIAP) and limocitrin significantly increased cleaved PARP, caspase-3, and -8 expression compared to the control group (Fig. 6C–H).

Discussion

Despite numerous breakthroughs in its identification and treatment, oral cancer remains a major threat to worldwide public health[10]. Oral cancer patients have a poor (50%) 5-year survival rate because of their vulnerability to metastasis[11]. Natural anti-cancer medications have demonstrated less adverse effects than

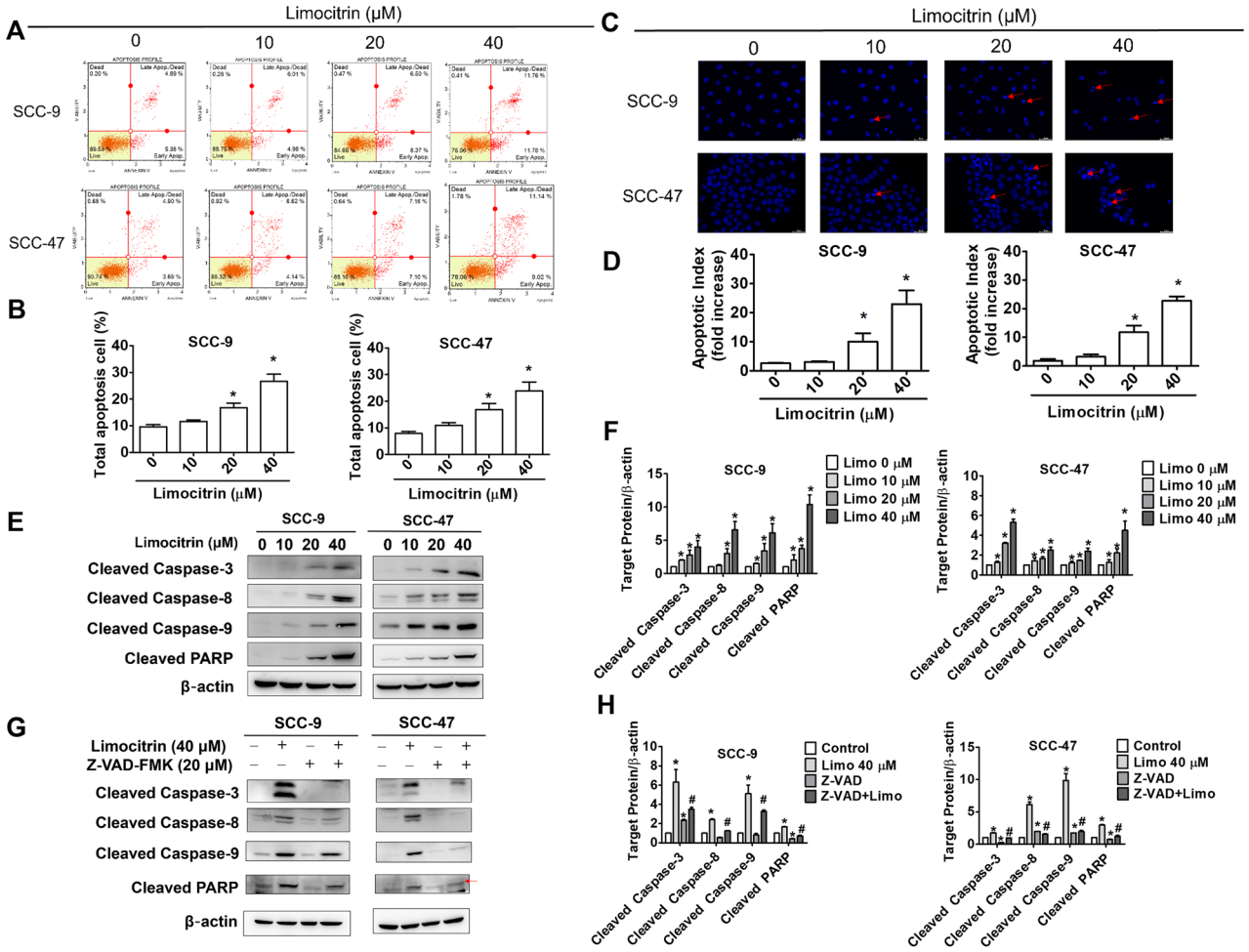

Fig. 4. Induction of caspase-related apoptosis in oral cancer cells by limocitrin. SCC-9 and SCC-47 cells were treated with limocitrin for 24 h. (**A**) Annexin-V/propidium iodide double staining for apoptosis detection. (**B**) Proportion of apoptotic cells. (**C**, **D**) Chromatin condensation was assessed using DAPI staining following the treatment of cells with limocitrin (0, 10, 20, and 40 μM) for 24 h. Scale bar = 50 μm. White arrows denote chromatin condensation. (**E**) Western blot analysis of cleaved caspases and PARP, with β-actin as the internal control. (**F**) Protein expression levels are displayed graphically. (**G**) Cells were pretreated with the caspase inhibitor, Z-VAD-FMK, and then with limocitrin for 24 h, with β-actin as the internal control. (**H**) Quantitation of cleaved caspase-related proteins and PARP is illustrated. All data are presented as mean ± standard deviation (n = 3). *$p < 0.05$, indicating statistical significance compared with the control group.

chemotherapy medications. These restrictions motivate future studies to concentrate on creating stronger medicinal medications derived from natural sources. It has been demonstrated that limocitrin, a flavonol glycoside, inhibits the activity of several enzymes, such as phosphodiesterase (https://www.biosynth.com/p/XL173020/489-33-8-limocitrin). It also possess anti-inflammatory and anti-cancer properties. Based on previous study, limocitrin has an anti-proliferative and pro-apoptotic effect on breast cancer cells[8]. Limocitrin greatly reduced breast cancer cells viability, with IC50 values of 29.33 ± 0.010 and 28.70 ± 0.030 μM for MDA-MB-231 and MCF-7 cells, respectively[8]. Our previous study showed that[9], limocitrin treatment increased the cytotoxicity of KHYG-1 cells against K562 cells, thereby altering the MAPK pathway. Nevertheless, the anticancer activity of limocitrin in oral cancer is not completely explored. In the present study, we examined the cellular mechanism of limocitrin's anticancer effects on oral cancer cells.

In this study, an effective dose of limocitrin to inhibit SCC-9 was found to be 40 μM at 48 h and 72 h treatment, whereas in SCC-47 cells, 40 μM can inhibit only 40% of cell viability until 72 h treatment. However, no significant difference was observed between the effective dose (40 μM) of limocitrin at 48 h and 72 h in both oral cancer cells. We also performed a colony formation assay to further confirm that limocitrin can inhibit the proliferation of oral cancer cells. Results showed that limocitrin exerts a strong anti-proliferative effect on oral cancer cells in a concentration-dependent manner (Fig. 1D,E). According to our results, SCC-9 cells treated with limocitrin showed a better cell inhibitory effect than SCC-47 cells.

Apoptosis and mitochondrial depolarization are mostly mediated by the pro-apoptotic Bcl-2 family proteins Bak and Bax, whereas Bcl-2 and Bcl-XL function as anti-apoptotic proteins[12]. In the present study, limocitrin-induced apoptosis in SCC-9 and SCC-47 cells correlated with a breakdown of mitochondrial membrane

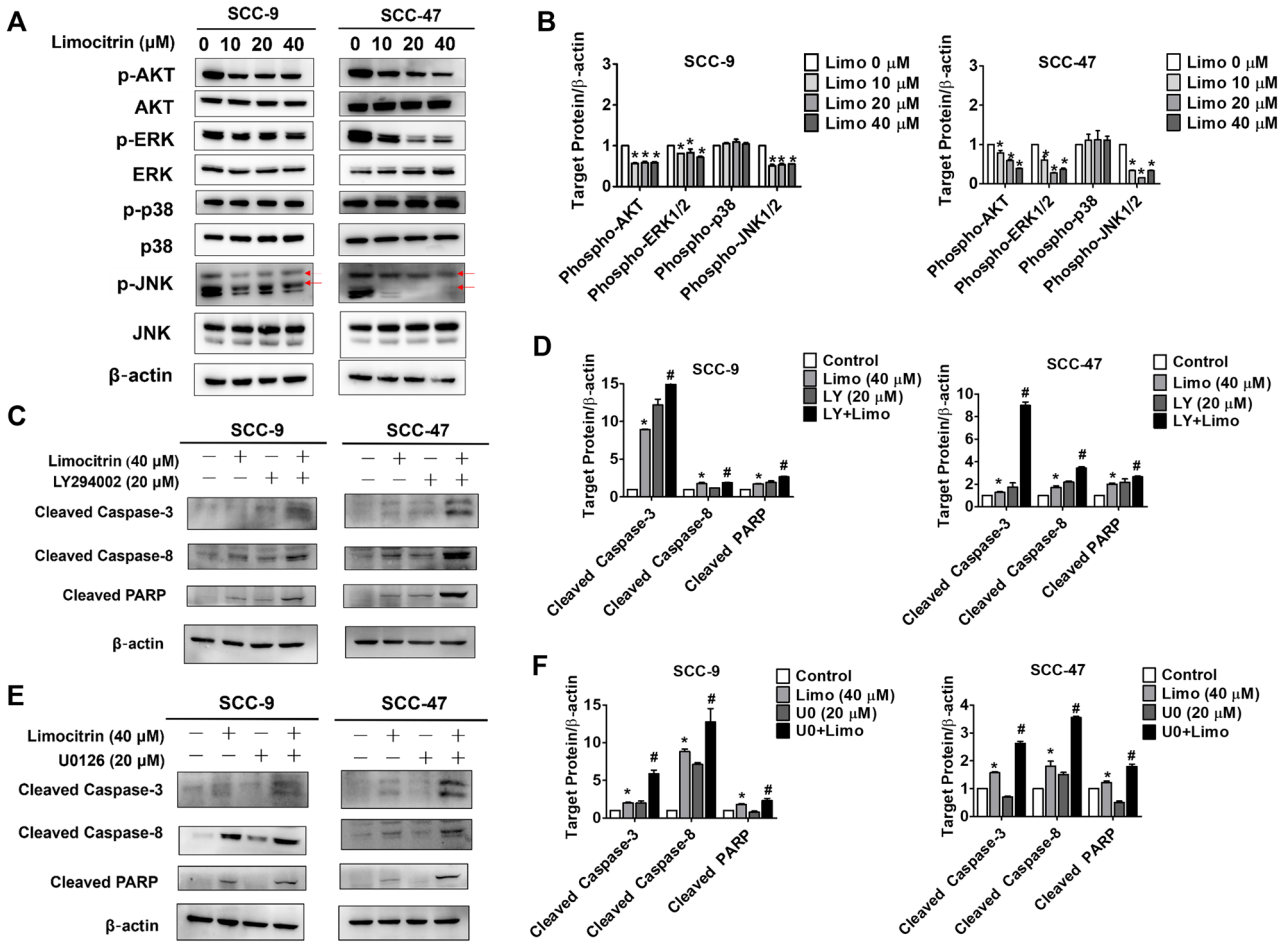

Fig. 5. Modulation of apoptosis in oral cancer cells by limocitrin through MAPK pathways. (**A**) Western blot assessment of phosphorylated AKT, ERK1/2, p38, and JNK1/2, with β-actin as the internal control. (**B**) Expression levels displayed as mean ± standard deviation (n = 3). *$p < 0.05$, indicating statistical significance compared with the control group. (**C**, **D**) Oral cancer cells were pretreated with the AKT inhibitor, LY294002, for 1 h and then treated with limocitrin for 24 h. Quantitation of cleaved caspase-3 and caspase-8 is illustrated. (**E**, **F**) Oral cancer cells were pretreated with the ERK inhibitor, U0126, for 1 h and then treated with limocitrin for 24 h. Quantitation of cleaved caspase-3 and caspase-8 is illustrated. All data are displayed as mean ± standard deviation (n = 3). *$p < 0.05$, indicating statistical significance compared with the control group. #$p < 0.05$, indicating statistical significance compared with limocitrin treatment alone.

potential, a slight increase in protein levels of BAX and BAK expression, and downregulation of Bcl-2 and Bcl-XL protein levels. Eight death domain-containing receptors, including TNFR1 (also known as DR1), Fas (also known as DR2), DR3, DR4, DR5, DR6, NGFR, and EDAR, are members of the TNFR superfamily. The death domain of these receptors attracts different proteins that mediate cell death and proliferation when they interact with their respective ligands. Decoy receptors (DcR1, DcR2, DcR3, and OPG) negatively influence receptor function[13]. Our data showed that limocitrin slightly increased Fas and DR5 expression in both the cancer cells; however, decoy receptor -DcR3 was greatly increased in limocitrin-treated SCC-9 cells. In SCC-47 cells, limocitrin treatment significantly increased DcR2 expression more than DcR3 expression.

High levels of mutation in cell cycle-encoded genes cause cancer cells to proliferate uncontrollably[14]. Consequently, therapeutic medications that specifically target cell cycle components, like cyclin inhibitors, are regarded as crucial pharmacological options. In terms of mechanism, limocitrin's impact on cell cycle arrest might be the key factor that halts the growth of tumors. In the present study, limocitrin inhibits the cell cycle and arrests cancer cells in the G2/M phase. Cyclin E1 and E2 are regulatory subunit proteins, while CDK2, CDK4, and CDK6 are cyclin-dependent kinases (CDKs) that are essential for the cell cycle[15]. Our data show that limocitrin potently downregulated Cyclin E1, E2, CDK2, CDK4, and CDK6 expression levels. An essential tumor suppressor is the protein p21 Waf1/Cip1, which is thought to be a promiscuous inhibitor of all cyclin complexes and cyclin-dependent kinases[16]. Our results showed that p21 was significantly upregulated in limocitrin-treated SCC-9 and SCC-47 at all exposure times. According to our findings, oral cancer cells treated with limocitrin had higher levels of p21 expression. Thus, it's possible that limocitrin triggered the p21-mediated G2/M arrest.

In addition, our study found that limocitrin induced cleaved caspase-3, caspase-8, caspase-9, and PARP expression, indicating the conversion of these caspases into active forms, implying that the intrinsic apoptotic

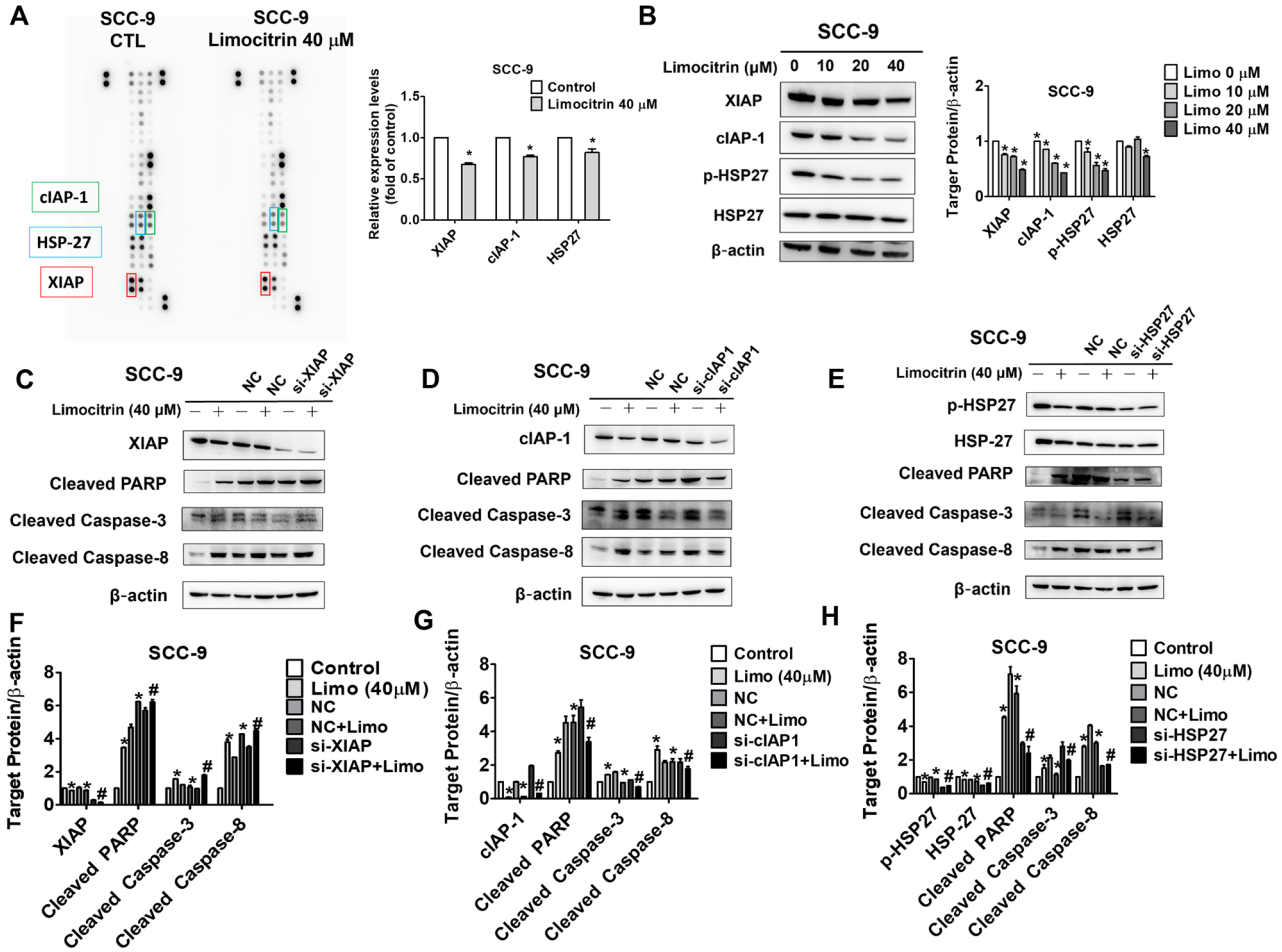

Fig. 6. Role of XIAP in limocitrin -induced apoptosis activation. (**A**) Reduced XIAP expression observed in SCC-9 and SCC-47 cells after 24 h of limocitrin treatment. (**B**) Quantitative analysis of XIAP, cIAP-1, p-HSP27 and HSP27 levels in SCC-9 and SCC-47 cell lines. (**C**, **F**) Cotreatment of SCC-9 with siRNA negative control (si-NC), XIAP siRNA (si-XIAP), and limocitrin. Quantitation of cleaved PARP, caspase-3, and caspase-8 is illustrated. (**D**, **G**) Cotreatment of SCC-9 with cIAP-1 siRNA (si-cIAP1) and limocitrin. Quantitation of cleaved PARP, caspase-3, and caspase-8 is illustrated. (**E**, **H**) Cotreatment of SCC-9 with HSP27 siRNA (si-HSP27) and limocitrin. Quantitation of cleaved PARP, caspase-3, and caspase-8 is illustrated. All data are displayed as mean ± standard deviation (n = 3). $^{*}p < 0.05$, indicating statistical significance compared with the control group. $\#p < 0.05$, indicating statistical significance compared with limocitrin treatment alone.

mechanism has been activated[17]. These results were further confirmed using the caspase inhibitor (Z-VAD-FMK). Oral cancer cells pretreated with Z-VAD-FMK decreased cleaved caspase-3, caspase-8, caspase-9, and PARP expression, which were reversed after limocitrin treatment. In our study, limocitrin administration caused apoptosis in SCC-9 cells by upregulating the expression of cleaved caspase-3 and caspase-9, whereas in SCC-47 cells, it caused apoptosis by upregulating the expression of cleaved caspase-8 and caspase-9.

Increased cleaved caspase-9 expression prompted us to investigate its upstream protein, AKT, a crucial enzyme that controls gene transcription, migration, and cell survival[18]. MAPK pathway signaling can influence a variety of biological processes in eukaryotic cells and, through transducing extracellular signals, regulate many cellular functions, such as migration, differentiation, and proliferation[19–22]. JNK[23], ERK, and p38 MAPK[24] proteins make up the MAPKs family, and each one is crucial for triggering caspases during apoptosis. As shown in Fig. 5A, results revealed that limocitrin frequently down-regulated the expression of phosphorylated AKT and ERK1/2 expression. These findings collectively indicate that the limocitrin-induced apoptosis of oral cancer cells is associated with the inhibition of the AKT/ERK pathway. Next, we used selective inhibitors of AKT (LY294002) and ERK (U0126) to determine which of these proteins was the main mediator of limocitrin-induced apoptosis in oral cancer cells. Limocitrin-inhibited ERK is required for the activation of caspase-8, caspase-3, and PARP cleavage. Together, our results suggest that blocking ERK signaling could be a better strategy for enhancing limocitrin-induced apoptosis in oral cancer cells.

In the present study, we investigated the role of the IAP family members in the oral cancer cell line. Compared with the control group, cells treated with limocitrin decreased cIAP-1, XIAP, and HSP-27 protein expression. In addition, we wanted to find out if IAP knockdown could make oral cancer cells more susceptible to apoptosis

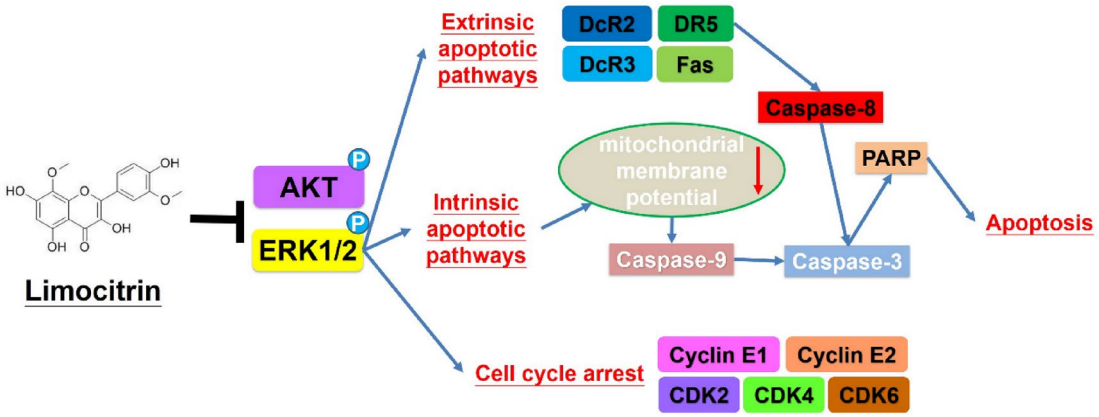

Fig. 7. The schematic diagram of limocitrin-induced apoptosis in oral cancer cells.

and how much each of cIAP-1, XIAP, and HSP-27 contributes to this process. Protein-level knockdown of cIAP-1, XIAP, and HSP-27, either separately or in combination, was further assessed by western blotting (Fig. 6C–E), which showed a notable decrease in the targeted protein. Si-XIAP decreased cleaved caspase-3 expression. XIAP directly inhibits the activity of caspase-3 expression to induce the apoptotic cascade[25]. Furthermore, XIAP knockdown decreased cleaved PARP, caspase-3, and caspase-8, which was reversed after limocitrin treatment. This data suggests that limocitrin induced apoptosis by inhibiting XIAP expression and by inducing cleaved caspase-3 and -8 expression.

In conclusion, our results reveal a unique action mechanism of limocitrin on ERK signaling pathways (Fig. 7). Limocitrin triggers cell apoptosis by inducing Bak, Bax and decreasing Bcl2 and Bcl-xL expression; it may lead to cell cycle arrest at the G2/M phase by inhibiting the activity of cell cycle proteins such as cyclin E1, E2, CDK2, CDK4, and CDK6, thereby increasing p21 expression. Limocitrin treatment significantly decreased ERK phosphorylation and further combination of ERK inhibitor (U0126) with limocitrin-induced cleaved caspase-3, -8, and PARP expression in both SCC-9 and SCC-40 cell lines. Limocitrin induced apoptosis in oral cancer cells by inhibiting XIAP expression, which further induced caspase-3 and caspase-8 expression. These findings highlight the potential of G-Rh2 as a therapeutic agent for the treatment of oral cancer.

Data availability

The data used to support the findings of this study are available from the corresponding author upon request.

Received: 18 December 2024; Accepted: 12 May 2025
Published online: 22 May 2025

References

1. Omar, E. Current concepts and future of noninvasive procedures for diagnosing oral squamous cell carcinoma—a systematic review. *Head Face Med.* **11**, 6 (2015).
2. Güneri, P. & Epstein, J. B. Late stage diagnosis of oral cancer: Components and possible solutions. *Oral. Oncol.* **50**(12), 1131–1136 (2014).
3. Lenoci, D. et al. Oral cancer in young adults: Incidence, risk factors, prognosis, and molecular biomarkers. *Front. Oncol.* **14**, 1452909 (2024).
4. Comprehensive genomic characterization of squamous cell lung cancers, *Nature* **489**(7417), 519–25 (2012).
5. Papa, S., Choy, P. M. & Bubici, C. The ERK and JNK pathways in the regulation of metabolic reprogramming. *Oncogene* **38**(13), 2223–2240 (2019).
6. Ye, B., Ma, J., Li, Z., Li, Y. & Han, X. Ononin shows anticancer activity against laryngeal cancer via the inhibition of ERK/JNK/p38 signaling pathway. *Front. Oncol.* **12**, 939646 (2022).
7. Thai, Q. D. et al. Phytochemical study and biological evaluation of chemical constituents of *Platanus orientalis* and Platanus x acerifolia buds. *Phytochemistry* **130**, 170–181 (2016).
8. Lim, H.-J. et al. Limocitrin suppresses breast cancer through inducing apoptotic-cell death signaling and inhibiting the PI3K/AKT/mTOR/S6K cell survival signaling. *J. Med. Food* **26**(10), 749–759 (2023).
9. Hsieh, M.-J. et al. Limocitrin increases cytotoxicity of KHYG-1 cells against K562 cells by modulating MAPK pathway. *Environ. Toxicol.* **38**(12), 2939–2951 (2023).
10. Kannan, K., Pitchiah, S. & Ramasamy, P. Novel therapeutic inhibitors for oral squamous cell cancer (OSCC) from seaweeds, European journal of surgical oncology: The journal of the European Society of Surgical Oncology and the British Association of. *Surg. Oncol.* **49**(5), 1048–1049 (2023).
11. Zhao, F., Xu, D., Wang, X. & Wang, X. FNDC5 affects invasion and migration of oral cancer by inhibiting PI3K/Akt/Snail signaling pathway. *Sci. Rep.* **14**(1), 26881 (2024).
12. Qian, S. et al. The role of BCL-2 family proteins in regulating apoptosis and cancer therapy. *Front. Oncol.* **12**, 985363 (2022).
13. Ge, Z., Sanders, A. J., Ye, L. & Jiang, W. G. Aberrant expression and function of death receptor-3 and death decoy receptor-3 in human cancer. *Exp. Ther. Med.* **2**(2), 167–172 (2011).
14. Otto, T. & Sicinski, P. Cell cycle proteins as promising targets in cancer therapy. *Nat. Rev. Cancer* **17**(2), 93–115 (2017).
15. Suski, J. M., Braun, M., Strmiska, V. & Sicinski, P. Targeting cell-cycle machinery in cancer. *Cancer Cell* **39**(6), 759–778 (2021).
16. Salanci, Š et al. The induction of G2/M phase cell cycle arrest and apoptosis by the chalcone derivative 1C in sensitive and resistant ovarian cancer cells is associated with ROS generation. *Int. J. Mol. Sci.* **25**(14), 7541 (2024).

17. Razali, N. S. C. et al. Curcumin piperidone derivatives induce caspase-dependent apoptosis and suppress miRNA-21 expression in LN-18 human glioblastoma cells. *Genes Environ.* **46**(1), 4 (2024).
18. Qi, S.-Z. et al. Phenylpropanoid-conjugated pentacyclic triterpenoids from the whole plants of Leptopus lolonum induced cell apoptosis via MAPK and Akt pathways in human hepatocellular carcinoma cells. *Bioorg. Chem.* **111**, 104886 (2021).
19. Guo, X., Ding, X. & Dong, J. Dichotomy of the BSL phosphatase signaling spatially regulates MAPK components in stomatal fate determination. *Nat. Commun.* **13**(1), 2438 (2022).
20. Kent, O. A. et al. Haploinsufficiency of RREB1 causes a Noonan-like RASopathy via epigenetic reprogramming of RAS-MAPK pathway genes. *Nat. Commun.* **11**(1), 4673 (2020).
21. Bragelmann, J. et al. MAPK-pathway inhibition mediates inflammatory reprogramming and sensitizes tumors to targeted activation of innate immunity sensor RIG-I. *Nat. Commun.* **12**(1), 5505 (2021).
22. Sui, X. et al. p38 and JNK MAPK pathways control the balance of apoptosis and autophagy in response to chemotherapeutic agents. *Cancer Lett.* **344**(2), 174–179 (2014).
23. Lan, Y.-Y. et al. Role of JNK activation in paclitaxel-induced apoptosis in human head and neck squamous cell carcinoma. *Oncol. Lett.* **22**(4), 705 (2021).
24. Schrantz, N. et al. p38-mediated regulation of an Fas-associated death domain protein-independent pathway leading to caspase-8 activation during TGFβ-induced apoptosis in human burkitt lymphoma B Cells BL41. *Mol. Biol. Cell* **12**(10), 3139–3151 (2001).
25. Scott, F. L. et al. XIAP inhibits caspase-3 and -7 using two binding sites: Evolutionarily conserved mechanism of IAPs. *EMBO J.* **24**(3), 645–655 (2005).

Acknowledgements

This study was supported by grants from National Science Council, Taiwan (MOST 111-2314-B-371-008-MY3) and Changhua Christian Hospital, Taiwan (112-CCH-IRP-003). The authors of the manuscript do not have a direct financial relation with the commercial identity mentioned in this paper.

Author contributions

Author contributions: Bharath Kumar Velmurugan: Conceptualization (equal); Writing—Original draft preparation (equal). Chia-Chieh Lin: Methodology (equal); Software (equal); Min-Yun Kao: Methodology (equal); Software (equal). Hsin-Yu Ho: Conceptualization (equal); Writing—review & editing (equal). Yi-Ching Chuang: Methodology (equal); Software (equal). Yu-Sheng Lo: Methodology (equal); Software (equal). Ming-Ju Hsieh: Conceptualization (equal); Writing—Original draft preparation (equal); Writing—review & editing (equal).

Funding

This research received no external funding.

Declarations

Competing interest

The authors declare no competing interests.

Additional information

Supplementary Information The online version contains supplementary material available at https://doi.org/10.1038/s41598-025-02178-6.

Correspondence and requests for materials should be addressed to M.-J.H.

Reprints and permissions information is available at www.nature.com/reprints.

Publisher's note Springer Nature remains neutral with regard to jurisdictional claims in published maps and institutional affiliations.

Open Access This article is licensed under a Creative Commons Attribution-NonCommercial-NoDerivatives 4.0 International License, which permits any non-commercial use, sharing, distribution and reproduction in any medium or format, as long as you give appropriate credit to the original author(s) and the source, provide a link to the Creative Commons licence, and indicate if you modified the licensed material. You do not have permission under this licence to share adapted material derived from this article or parts of it. The images or other third party material in this article are included in the article's Creative Commons licence, unless indicated otherwise in a credit line to the material. If material is not included in the article's Creative Commons licence and your intended use is not permitted by statutory regulation or exceeds the permitted use, you will need to obtain permission directly from the copyright holder. To view a copy of this licence, visit http://creativecommons.org/licenses/by-nc-nd/4.0/.

© The Author(s) 2025